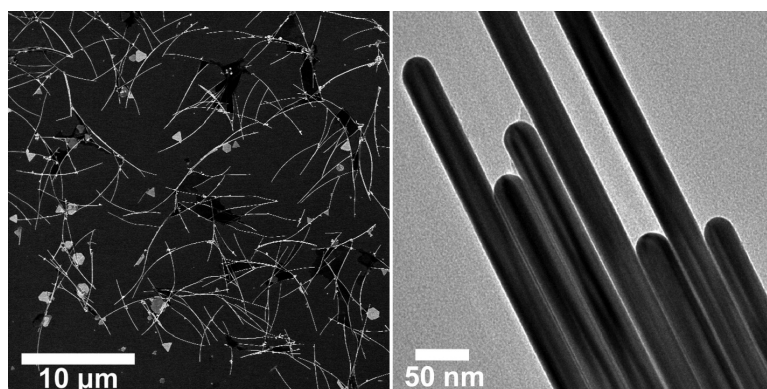


## Chemical Synthesis of Gold Nanowires in Acidic Solutions

Franklin Kim, Kwonnam Sohn, Jinsong Wu, and Jiaying Huang

*J. Am. Chem. Soc.*, **2008**, 130 (44), 14442-14443 • DOI: 10.1021/ja806759v • Publication Date (Web): 14 October 2008

Downloaded from <http://pubs.acs.org> on February 8, 2009



### More About This Article

Additional resources and features associated with this article are available within the HTML version:

- Supporting Information
- Access to high resolution figures
- Links to articles and content related to this article
- Copyright permission to reproduce figures and/or text from this article

[View the Full Text HTML](#)

## Chemical Synthesis of Gold Nanowires in Acidic Solutions

Franklin Kim, Kwonnam Sohn, Jinsong Wu, and Jiaying Huang\*

Department of Materials Science and Engineering, Northwestern University, Evanston, Illinois 60208-3108

Received August 27, 2008; E-mail: jiaying-huang@northwestern.edu

Gold nanowires with well-defined crystallographic surfaces could serve as a model system for studies like plasmonic waveguides<sup>1</sup> and tip enhanced Raman spectroscopy.<sup>2</sup> While much success has been achieved in making single crystalline (or multiply twinned) nanowires of other fcc metals including Ag<sup>3,4</sup> and Cu,<sup>5</sup> such gold nanowires have long been a missing piece in the toolbox of plasmonics nanomaterials. Various methods such as lithography<sup>6</sup> and templated synthesis<sup>7,8</sup> have been reported for making gold nanowires. However, such nanowires were usually polycrystalline in nature and/or have less defined surfaces. To the best of our knowledge, the synthesis of well-defined Au nanowires has been limited to those with either very large ( $>100$  nm<sup>9</sup>) or ultrathin diameters ( $<2$  nm<sup>10,11</sup> and  $<10$  nm<sup>12</sup>). Here we report a room temperature acidic solution route to synthesize gold nanowires with diameters tunable between 16 and 66 nm and lengths up to 10  $\mu$ m.

Our synthetic method was based on the well-known three-step seeding synthesis that was originally developed for preparing gold nanorods.<sup>13</sup> First, 3–4 nm seed particles are prepared by rapid reduction of a gold precursor (i.e., HAuCl<sub>4</sub>) with a strong reducing agent (e.g., NaBH<sub>4</sub>). Then the seed particles are added to a growth solution containing HAuCl<sub>4</sub>, ascorbic acid, and hexadecyl-trimethylammonium bromide (CTAB).<sup>14</sup> Ascorbic acid rapidly reduces the gold salt from its Au(III) to Au(I) state, leading to a colorless, meta-stable solution at room temperature. The addition of seeds induces *in situ* autocatalytic reduction of Au(I), thus enlarging the seed particles. CTAB is used as a structural directing agent for producing nanorods, likely due to the stabilization of the side surface from preferential adsorption on the (100) surface.<sup>15</sup> The diameters of such made gold nanorods were typically less than 10 nm with an aspect ratio smaller than 10.<sup>13,14</sup> Later a three-step seeding approach was reported to yield nanorods with an aspect ratio of up to 18.5,<sup>13</sup> which was further extended to  $>20$ .<sup>16,17</sup> Thus it appears that longer nanorods can be obtained if one can further extend the growth. In an analogy to radical polymerization, if the number of the initiator sites (seed) is reduced, a longer polymer chain (nanowires) should be obtained. Therefore, we set out to do synthesis using significantly less seeds. We also discovered that nanowire growth was promoted in acidic solution. By combining the two factors, we were able to greatly increase the aspect ratio of the products to over 200.

The as-made nanowires can be easily observed under an optical microscope due to strong scattering (Figure 1a),<sup>18</sup> which would be very difficult for the ultrathin nanowires.<sup>10–12</sup> The brighter wires were found to be bundles of two or more nanowires when observed under SEM. The ease of optical microscope observation opens up the possibility of micromanipulating for further studies on individual nanowires. The lengths of the nanowires reached up to 10  $\mu$ m, which was confirmed by SEM (Figure 1b). The diameter of the nanowires was found to be  $\sim 31.5$  nm based on TEM analysis (Figure 1c). The wires have sharp tips that may make them potentially useful for tip enhanced Raman spectroscopy.<sup>2</sup> Electron diffraction patterns were acquired from multiple individual nanowires,

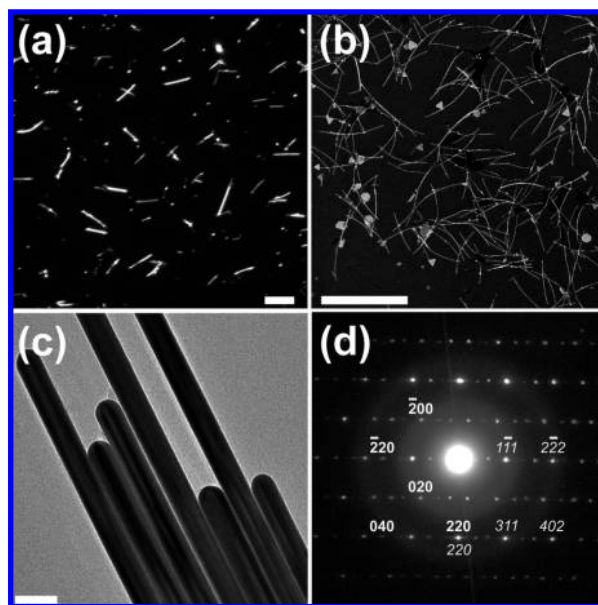


**Figure 1.** Gold nanowires produced by a three-step seeding method in acidic growth solution. (a) Dark-field optical microscopy, (b) SEM, (c) TEM, and (d) selective-area electron diffraction (SAED). (d) Interpenetrating  $\langle 112 \rangle$  and  $\langle 100 \rangle$  zone patterns, distinguished by italics and bold typeface, respectively. The scale bars represent 10  $\mu$ m in (a) and (b), and 100 nm in (c).

ires, all of which show interpenetrated two sets of patterns similar to Figure 1d, which is an overlap of the  $\langle 112 \rangle$  and  $\langle 100 \rangle$  zone patterns from an *fcc* structure.<sup>15</sup> Such patterns have been observed with short Au nanorods, and nanowires of other *fcc* metals (e.g., Ag, Cu), all of which have pentagonal cross-sections and are multiply twinned along the long axis.<sup>4,5</sup> Our Au nanowires have the same  $\langle 110 \rangle$  growth direction along their long axis with the sides bound with the  $\{100\}$  surface.

The length and the diameter of the nanowires can be tuned by controlling the seed concentration and pH of the growth solution. Figure 2 and S2 show the SEM and TEM images of nanowires produced with various amounts of seed solution and pH values. In a pH = 1 growth solution, nanowires with lengths of  $\sim 1$ –2  $\mu$ m (Figure 2a) were obtained. As expected, longer nanowires of 7–10  $\mu$ m in length were indeed obtained with less seeds (200  $\mu$ L) (Figure 2b). However, when the seed volume was further reduced (20  $\mu$ L), the lengths of the resulting nanowires decreased to  $\sim 5$ –7  $\mu$ m (Figure 2c). Meanwhile, we observed an increase in the amount of byproduct—irregularly shaped particles and flakes. These types of particles were also obtained in control experiments where the growth solution itself was allowed to age for several hours (Figure S2a, S2b). This suggests that there were competing self-nucleated side reactions along with the seed catalyzed wire-forming reaction. Therefore, the optimal amount of the seeds for producing long nanowires should be on the order of a few hundreds of microliters.

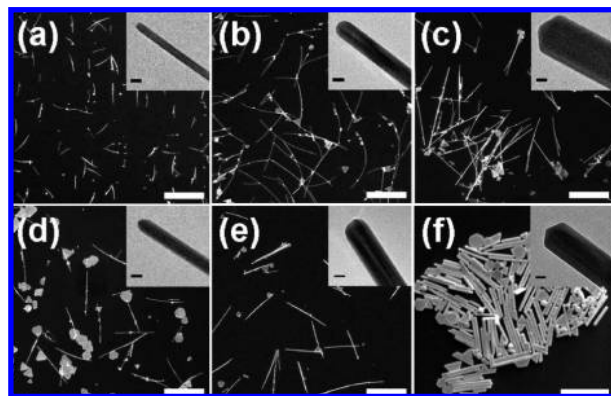


**Figure 2.** SEM and TEM (insets) images showing the effects of the seed (a–c) and acid (b, d–f) concentrations on the gold nanowire products. In (a–c), the volume of added  $\text{HNO}_3$  was kept constant at  $100 \mu\text{L}$  ( $\text{pH} = 1.15$ ). (a)  $2 \text{ mL}$ , (b)  $200 \mu\text{L}$ , and (c)  $20 \mu\text{L}$  of seed solutions were added to  $22.5 \text{ mL}$  of final growth solution, respectively. In (d–f) the volume of seed solution was kept constant at  $200 \mu\text{L}$ . (d)  $200 \mu\text{L}$ , (e)  $50 \mu\text{L}$ , and (f)  $0 \mu\text{L}$  of  $\text{HNO}_3$  were added to the final growth solution, respectively. Scale bars for SEM images are  $5 \mu\text{m}$ , except in (f) where it represents  $1 \mu\text{m}$ . Black scale bars in TEM images represent  $20 \text{ nm}$ .

The seed concentration also affected the diameters of the products. When the seed volume was reduced from  $2 \text{ mL}$ ,  $200$  to  $20 \mu\text{L}$ , the diameters increased from  $\sim 16 \text{ nm}$ ,  $32$  to  $66 \text{ nm}$ , respectively (Figure 2, insets).

Figure 2d, b, e, and f show nanowires produced by changing the volume of  $\text{HNO}_3$  from  $200 \mu\text{L}$ ,  $100 \mu\text{L}$ ,  $50 \mu\text{L}$ , to  $0 \mu\text{L}$  (no addition), respectively, while keeping the amount of seed constant ( $200 \mu\text{L}$ ). With  $200 \mu\text{L}$  of  $\text{HNO}_3$  ( $\text{pH} = 0.8$ ), the growth solution quickly gelled and the resulting products were microplatelets and nanowires of  $4\text{--}5 \mu\text{m}$  in length (Figure 2d). The longest nanowires with best yield were obtained using  $100 \mu\text{L}$  of  $\text{HNO}_3$  ( $\text{pH} = 1.1$ ) in the synthesis (Figure 2b). Shorter nanowires were produced with less  $\text{HNO}_3$  (Figure 2e,  $\text{pH} = 1.4$ ). Without  $\text{HNO}_3$  ( $\text{pH} = \sim 4$ ), only thick nanorods ( $> 50 \text{ nm}$ ) with submicron lengths were obtained. The average diameter of the wires increased with a decreased amount of  $\text{HNO}_3$ . From Figure 2d, b, e, to f, the average diameters increased from  $29$ ,  $32$ ,  $44$ , to  $56 \text{ nm}$ , respectively. In summary, the general trend observed was that less seed led to thicker and longer wires, whereas lower  $\text{pH}$  (when  $> 1$ ) gave thinner and longer wires. By tuning these two parameters, gold nanowires with different diameters and lengths can be made.

The growth of nanowires was favored in acidic solutions even without seeds. The growth solution itself only produced irregularly shaped particles upon aging (Figure S2a). However, with the addition of nitric acid, a small amount of nanowires started to appear (Figure S2b). The role of acid was further investigated by replacing  $\text{HNO}_3$  with  $\text{HCl}$ ,  $\text{H}_2\text{SO}_4$ , and  $\text{NaNO}_3$ . Similar results were obtained with  $\text{HCl}$ . For the diprotic  $\text{H}_2\text{SO}_4$ , comparable results were obtained but only at half of the concentrations needed for the monoprotic  $\text{HCl}$  or  $\text{HNO}_3$ . With  $\text{NaNO}_3$  the products were similar to those obtained without acid. This suggests that it was indeed the low  $\text{pH}$  value, rather than the counterions that promoted the nanowire growth.

The nanowire synthesis was often accompanied by the formation of particles and plates that were likely initiated by competing unseeded homogeneous nucleation. Since seeds can lower the nucleation energy barrier, the seeded reaction will proceed faster than the unseeded ones. Therefore, the yield of the nanowires should be higher when the  $\text{Au(I)}$  to  $\text{Au(0)}$  reaction is suppressed. This

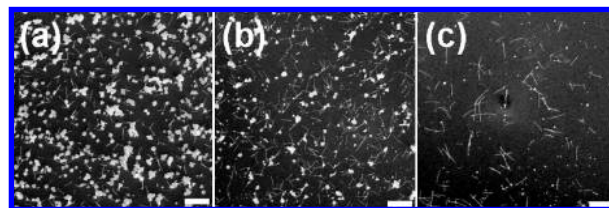


**Figure 3.** SEM images of gold nanowires synthesized at different temperatures: (a)  $60$ , (b)  $30$ , and (c)  $20 \text{ }^\circ\text{C}$ . Scale bars =  $10 \mu\text{m}$ .

was achieved at lower reaction temperatures. Figure 3 shows samples prepared at  $60$ ,  $30$ , and  $20 \text{ }^\circ\text{C}$ . Indeed the amount of byproduct was significantly reduced at lower temperature.  $20 \text{ }^\circ\text{C}$  seemed to be the lower temperature limit due to the crystallization and precipitation of CTAB. This may also explain why nanowire growth was promoted by adding acid since the reduction rate was much lowered in acidic solutions.

In conclusion, gold nanowires with diameters  $20\text{--}50 \text{ nm}$  and aspect ratio over  $200$  can be produced by using a reduced amount of seeds in acidic growth solutions. These gold nanowires have a well-defined surface, thus filling the missing spot in the tool box of metal plasmonic nanostructures.

**Acknowledgment.** The work was supported by a Northwestern new faculty startup fund, and a seed grant from the MRSEC program of NSF (DMR #0520513) at Northwestern University. K.S. was partially supported by a 3M fellowship. SEM and TEM were performed in the EPIC facility of the NUANCE Center and the McCormick Laboratory for Manipulation and Characterization of Nano Structural Materials.

**Supporting Information Available:** Experimental details; TEM images of nanowires produced with various seed and  $\text{HNO}_3$  concentrations (Figure S2); SEM images of nanowires produced with  $\text{HCl}$ ,  $\text{H}_2\text{SO}_4$ , and  $\text{NaNO}_3$  (Figure S3); UV–vis spectrum of a nanowire solution (Figure S4). This material is available free of charge via the Internet at <http://pubs.acs.org>.

## References

- (1) Sanders, A. W.; Routenberg, D. A.; Wiley, B. J.; Xia, Y.; Dufresne, E. R.; Reed, M. A. *Nano Lett.* **2006**, *6*, 1822–1826.
- (2) Stockle, R. M.; Suh, Y. D.; Deckert, V.; Zenobi, R. *Chem. Phys. Lett.* **2000**, *318*, 131–136.
- (3) Jana, N. R.; Gearheart, L.; Murphy, C. J. *Chem. Commun.* **2001**, 617–618.
- (4) Sun, Y.; Gates, B.; Mayers, B.; Xia, Y. *Nano Lett.* **2002**, *2*, 165–168.
- (5) Chang, Y.; Lye, M. L.; Zeng, H. C. *Langmuir* **2005**, *21*, 3746–3748.
- (6) Krenn, J. R.; Weeber, J. C.; Dereux, A.; Bourillot, E.; Goudonnet, J. P.; Schider, B.; Leitner, A.; Aussenegg, F. R.; Girard, C. *Phys. Rev. B* **1999**, *60*, 5029–5033.
- (7) Dickson, R. M.; Lyon, L. A. *J. Phys. Chem. B* **2000**, *104*, 6095–6098.
- (8) Cross, C. E.; Hemminger, J. C.; Penner, R. M. *Langmuir* **2007**, *23*, 10372–10379.
- (9) Liu, X. G.; Wu, N. Q.; Wunsch, B. H.; Barsotti, R. J.; Stellacci, F. *Small* **2006**, *2*, 1046–1050.
- (10) Huo, Z.; Tsung, C.-k.; Huang, W.; Zhang, X.; Yang, P. *Nano Lett.* **2008**, *8*, 2041–2044.
- (11) Lu, X.; Yavuz, M. S.; Tuan, H.-Y.; Korgel, B. A.; Xia, Y. *J. Am. Chem. Soc.* **2008**, *130*, 8900–8901.
- (12) Wang, C.; Hu, Y.; Lieber, C. M.; Sun, S. *J. Am. Chem. Soc.* **2008**, *130*, 8902–8903.
- (13) Murphy, C. J.; San, T. K.; Gole, A. M.; Orendorff, C. J.; Gao, J. X.; Gou, L.; Hunyadi, S. E.; Li, T. *J. Phys. Chem. B* **2005**, *109*, 13857–13870.
- (14) Nikoobakht, B.; El-Sayed, M. A. *Chem. Mater.* **2003**, *15*, 1957–1962.
- (15) Johnson, C. J.; Dujardin, E.; Davis, S. A.; Murphy, C. J.; Mann, S. *J. Mater. Chem.* **2002**, *12*, 1765–1770.
- (16) Wu, H.-Y.; Huang, W.-L.; Huang, M. H. *Cryst. Growth Des.* **2007**, *7*, 831–835.
- (17) Wu, H.-Y.; Chu, H.-C.; Kuo, T.-J.; Kuo, C.-L.; Huang, M. H. *Chem. Mater.* **2005**, *17*, 6447–6451.
- (18) Lee, K.-S.; El-Sayed, M. A. *J. Phys. Chem. B* **2005**, *109*, 20331–20338.

JA806759V